

# OPTIMIZATION OF AN RF PROBE VICINITY FOR RF GUN CAVITIES

V.V. Paramonov\*, Institute for Nuclear Research of the RAS, Moscow, Russia

## Abstract

To provide electron bunches with exceptionally high brightness, RF gun cavity should operate with the extreme electric and magnetic fields. The RF probe is required for the mostly reliable and precise measurements of the RF field phase and amplitude directly from the cavity. The implementation of an RF probe in the cavity design generates a set of coupled problems, which is analyzed and compared for different operating frequencies and different RF pulse length. Both general dependencies and particularities are considered. Some recommendations for practical choice of the RF probe are presented.

## INTRODUCTION

RF gun cavities are intended for generation of high brightness electron bunches for Free Electron Lasers (FELs), based on linear accelerators. The normal conducting Fel's linacs operate in the S band frequency range with a relatively short length of RF pulse  $\tau$ . For FEL's based on superconducting technology the L band range is adopted with much more long RF pulse. Instead of a large variety particular technical solutions, The major part of existing gun cavities is based on BNL concept, [1], which is shown in Fig. 1 with modern solutions. A gun cavity consists of two cells, surrounded by cooling circuit in cavity walls. The length of cells is optimized to have a small emittance of the bunch. A photo cathode is placed in the first short cell

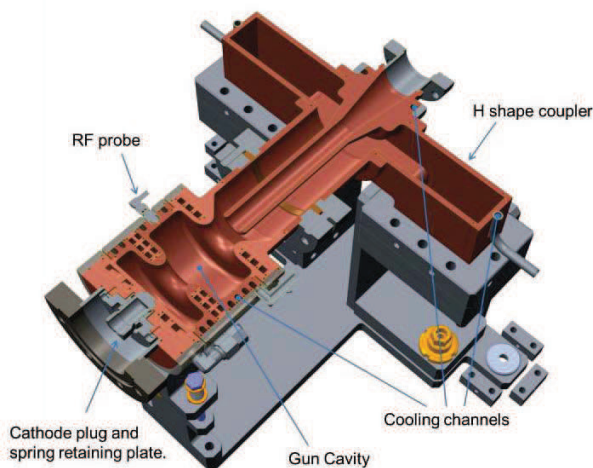


Figure 1: The modern design of RF gun cavity, [2].

of the cavity. For RF power input in Fig. 1 is shown the coaxial RF coupler to avoid an azimuthal nonhomogeneity of the cavity field. To provide electron bunches with an exceptionally high peak bunch current as well as a small transverse emittance, RF gun cavities should operate with

an extreme electric field at the photo cathode  $E_c$  and, hence, in the total cavity. To provide the required performance of the FEL facility, the phase of the RF field in the gun cavity should be controlled with a maximal possible precision for synchronization with the main linac RF system. An RF probe in the cavity cell provides perturbation in the gun cavity surface resulting in perturbation of the field distribution both in the nearest probe vicinity and in the total cavity volume. It leads to a set of coupled effects, which are estimated below. To point out particularities of the cavity operating regime we will the S mode as operation with frequency  $f_0 \approx 3 \text{ GHz}$ ,  $E_c \approx 115 \frac{\text{MV}}{\text{m}}$ ,  $\tau \approx 3 \mu\text{s}$  and L mode with parameters  $f_0 \approx 1.3 \text{ GHz}$ ,  $E_c \approx 60 \frac{\text{MV}}{\text{m}}$ ,  $\tau \approx 1000 \mu\text{s}$ .

## EQUIVALENT CAVITY

For the analysis we have to know with the high precision the field distributions in a small region, compared in dimensions with a probe hole. This case the details of the total cavity design are not so important. To have the dense mesh and the high precision in numerical simulations the equivalent sector cavity was considered together with the probe hole vicinity, Fig. 2a. Simulations were performed by using ANSYS software, [3].

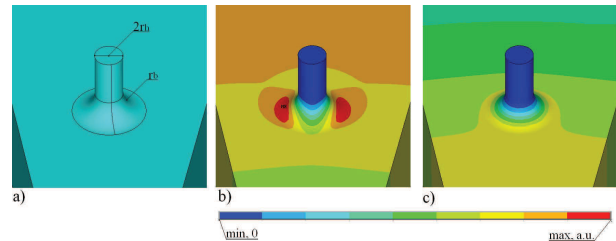


Figure 2: The equivalent cavity in with the RF probe hole, (a), and distributions of magnetic, (b), and electric, (c), fields intensity near the probe hole.

## VICINITY OF THE PROBE HOLE

The set of coupled effects is estimated below.

### *Perturbation of the field distribution*

Essential dimensions of the probe hole, the hole radius  $r_h$  and the radius of edge rounding  $r_b$  are shown in Fig. 2a. In the nearest vicinity the probe hole provides different perturbations in the distributions of electric and magnetic fields. For magnetic field the perturbation is like dipole addition, Fig. 2b, while for for electric field the perturbation is like monopole, Fig. 2c. Because the maximum values are interesting, let us consider the field enhancement,  $\frac{H_{max}}{H_0}$ ,  $\frac{E_{max}}{E_0}$ , where  $H_{max}$ ,  $E_{max}$  are the maximal values of field intensities in the probe vicinity and  $H_0$ ,  $E_0$  are the values of field

\* paramono@inr.ru

intensities in case of an unperturbed cavity. The simulated results of fields enhancement are presented in Fig. 3. Until

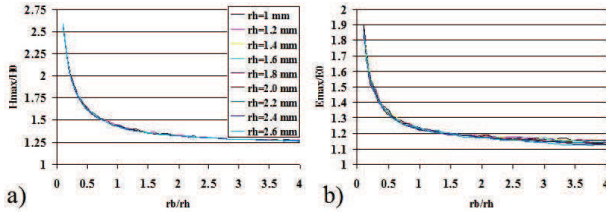


Figure 3: The plots of magnetic, (a), and electric, (b), fields enhancement in the probe vicinity.

the hole dimensions  $r_h, r_b \ll \frac{\lambda}{4}$ , where  $\lambda$  is the operating wavelength, the local field enhancement should depend on ratio  $\frac{r_b}{r_h}$  only. It is the sequence of a static approximation for distributions of fields near the small hole and in Fig. 3 one can see practically merged curves for different  $r_h$  values. With  $\frac{r_b}{r_h}$  increasing, for  $\frac{r_b}{r_h} \geq 1.5$ , the values for fields enhancement come to saturation and large  $r_b$  radius is not effective.

Together with a local perturbation of the field distribution in the nearest vicinity, the hole for the RF probe generates a field perturbation in the total cavity. The field  $\vec{E}$  in a slightly deformed cavity can be described, [4], as:

$$\vec{E} \approx \vec{E}_0 + \sum_{m \neq 0} \vec{E}_m \frac{\omega_m^2 \int_{\delta V} (Z_0^2 \vec{H}_m \vec{H}_n^* - \vec{E}_m \vec{E}_n^*) dV}{W_0(\omega_0^2 - \omega_m^2)}, \quad (1)$$

where  $Z_0 = \sqrt{\frac{\mu_0}{\epsilon_0}}$ ,  $\omega_m$ ,  $\vec{E}_m$ ,  $\vec{H}_m$  are the own frequencies and own fields of the modes in the unperturbed cavity,  $\delta V$  is the volume of perturbation and  $W_0$  is the stored energy of the fields. For the RF gun cavity the operating mode with symbol 0 in equation (1) is  $TM_{011}$  mode. The single hole couples with the operating mode all High Order Modes (HOM's) with azimuthal field dependence. For the cavity geometry, shown in Fig. 1 in the cavity spectrum below the cut off frequency of the RF coupler there are three dipole HOM's and just one quadrupole HOM with frequency  $f \approx 1.7f_0$ . With two symmetrically placed holes for dipole HOM's the coupling integral over one hole in (1) cancels the integral over the second hole and dipole additions in the field disappear. Simultaneously the addition from the quadrupole HOM doubles and only the way to reduce it is to decrease the value of the coupling integral in (1). Because the hole dimensions are much less as compared to a typical distance of field variation for all HOM's, we can rewrite (1) for this single quadrupole HOM as:

$$\vec{E} \approx \vec{E}_o + \frac{\omega_q^2 (Z_0^2 \vec{H}_{qh} \vec{H}_{0h}^* - \vec{E}_{qh} \vec{E}_{0h}^*)}{W_0(\omega_0^2 - \omega_q^2)} \delta V \vec{E}_q, \quad (2)$$

where  $\vec{H}_{qh}$  and  $\vec{E}_{qh}$  are the HOM fields at the RF probe position. The HOM's additions in the field distributions are proportional to  $\delta V$ , which rises fast,  $\delta V \sim r_h^3$  for  $\frac{r_b}{r_h} = const$  and for  $r_h = const$ ,  $\delta V \sim r_b^2$ , with increasing of hole dimensions.

## Pulsed RF heating

The RF heating effect takes place in RF gun cavities, resulting in significant temperature rise  $T_{sp}$  at the cavity surface during the RF pulse. For an approximation of the flat surface there is well known estimation, see [6]:

$$T_{sp} = \frac{2P_d \sqrt{\tau}}{\sqrt{\pi \rho k_c C_p}} = \frac{2P_d D_p}{\sqrt{\pi k_c}}, \quad D_p = \sqrt{\frac{k_c \tau}{\rho C_p}}, \quad (3)$$

where  $\rho$ ,  $k_c$ ,  $C_p$  are the density, heat conductivity and the specific heat for cavity material, which is, usually, OFHC copper, [6]. The diffusion length  $D_d$  is the effective length of heat propagation into cavity body. The temperature rise  $T_{sp}$  is proportional to RF loss density  $P_d$ . Since  $P_d \sim H_{max}^2$ , the local enhancement of magnetic field in the hole vicinity, Fig. 3a, leads to more sharp  $P_d$  increase, Fig. 4. For  $\frac{r_b}{r_h} \leq 1$  we have strong  $P_d$  enhancement, but with  $r_b$

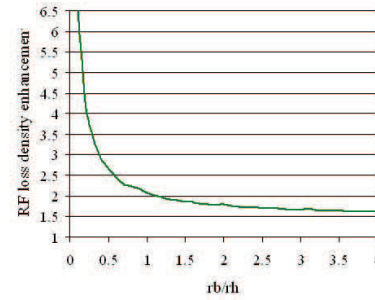


Figure 4: The plot of RF loss density enhancement.

increasing after  $\frac{r_b}{r_h} \geq 2$  there is no essential decrease in  $P_d$  value.

For the S operating mode the diffusion length for OFHC

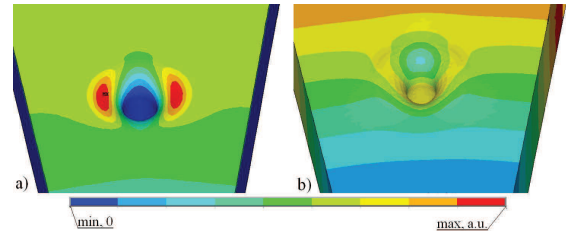


Figure 5: The distributions of the temperature rise  $T_{sp}$ , (a), and displacements, (b), in the vicinity of the hole, a.u.

copper  $D_d = 19 \mu m$  is much less than the dimensions of the probe hole. The estimation (3) works fine, the  $T_{sp}$  distribution at the cavity surface reflects  $P_d$  distribution and for induced thermal stress  $\sigma$  is valid well static approximation, [7]:

$$\sigma = \frac{\alpha E_{Ym} T_{sp}}{(1 - \nu)}, \quad (4)$$

where  $\alpha$ ,  $\nu$  and  $E_{Ym}$  are the thermal expansion, the Poisson's ratio and the elastic modulus for cavity material. For the operating L mode the diffusion length  $D_d$  is of  $\approx 340 \mu m$  and application of (3) and (4) is not so easy. Direct numerical simulations of the pulsed RF heating for L mode

were performed following to the procedure described in [5]. The simulated distributions for  $T_{sp}$  and displacements in the hole vicinity are shown in Fig. 4.

### Probe matching

For reliable RF measurements at the RF probe output the signal with RF power of  $P_p \sim 1 W$  is required. As compared to the total pulse RF power  $P_i \approx (6 \div 8) MW$ , dissipated in the cavity during RF pulse,  $P_p$  is the rather small value. We can consider the RF probe as the usual, but strongly mismatched RF coupler. Prescribing to the RF probe an equivalent external quality factor  $Q_e$ , from S parameters simulations we can define the required reflection coefficient  $S_{11}$  for this mismatched coupler:

$$Q_e = Q_0 \frac{P_i}{P_p}, S_{11} = \frac{Q_0 - Q_e}{Q_0 + Q_e} = \frac{P_i - P_p}{P_i + P_p} \approx 1 - \frac{2P_i}{P_p}, \quad (5)$$

where  $Q_0$  is the own quality factor of the cavity. The expected  $Q_e$  value for gun cavities is of  $\sim 10^{11}$  and simula-

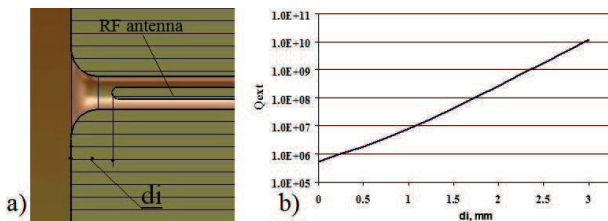


Figure 6: The model for  $S_{11}$  simulation, (a), and a typical  $Q_e(d_i)$  dependence on antenna immersion, (b).

tions of  $S$  parameters also are sensible on an equivalent cavity, Fig. 4a, with the scaling of results to the real gun cavity. In the probe hole fields are essential at the depth  $\sim r_b$ , see Fig. 2b,c. Into the cylindrical part of the hole fields decay as  $\approx \exp(-\frac{2.6 \cdot d_i}{r_h})$  both for S and L modes, as confirmed by the slope of the straight line of  $Q_e(d_i)$  dependence in Fig. 6b.

## DISCUSSION AND CONCLUSION

From physical reasons the probe hole dimensions should be small, but from mechanical reasons we can not select very small values and  $r_h \approx 1 mm$  is reasonable both for L and S modes. But recommended rounding value  $r_b$  differs for these modes. Due to the short RF pulse the pulsed heating effects are not strong for S mode and at the outer cavity wall  $T_{sp}$  is of  $\approx 10 K$ . The tolerable, safe, value, recommended in [6], is of  $T_{sp} \approx 40 K$ . We can allow for probe vicinity to be after RF pulse a hot spot at the surface and for the rounding  $r_b$  selection the ratio  $\frac{r_b}{r_h} \geq 0.5$  is tolerable. There are no limitations to place the RF probe at the outer cell surface, similar to Fig. 1.

For L mode the pulsed RF heating effects are much stronger due to the long RF pulse and after pulse already  $T_{sp} \approx 40 K$ , [5]. Near the RF probe  $T_{sp}$  value should not exceed such value at the other cavity parts. The RF probe can't be place at the outer wall of the cavity with close to

the maximal magnetic field. The probe should be moved to the front cavity wall with a lower  $|H|$  value, simultaneously selecting  $\frac{r_b}{r_h} \geq 1.5$  to restrict the local  $P_d$  enhancement. This case the diffusion length  $D_d$  is still much less than hole dimensions and expressions (3) and (4) work precisely. During the pulsed surface heating the value of the surface displacements is proportional to the heat deposited into the cavity body, [7], e.g.  $\sim \tau P_i$ . The simulated value of displacements with respect to unperturbed surface is of  $\approx (0.12 \div 0.15) \mu m$ , Fig. 5b. Taking into account  $Q_e(d_i)$  dependence, Fig. 6b, we have a rough estimate for relative precision of field amplitude measurement during RF pulse as  $\approx 0.1\%$ . For S mode this effect is two orders less.

For the RF probe matching in S mode a smaller immersion of antenna tip  $d_i$  is required due to a smaller scaling factor from equivalent cavity. With the tip immersion in the range  $1.0r_h \leq d_i \leq 2.5r_h$  the required RF power  $P_p$  can be obtained for both modes.

In ordinary simulations at the background of own numerical noises we can not distinguish the quadrupole addition in the cavity field. Just with noises filtering at the radius  $r = 0.043\lambda$  we detect for L mode the quadrupole additions in field components in the full cavity cell at the relative level  $\leq 1.3 \cdot 10^{-4}$  along and no addition above the level of  $\leq 1.0 \cdot 10^{-6}$  in the cathode cell. It is quite consistent with field distribution of the quadrupole HOM, coupled with operating mode by two holes. In S mode, for the same  $r_h, r_b$  values, the quadrupole addition is one order larger due to relative increasing of  $\frac{\delta V}{V}$  in (2).

For S mode restrictions for RF probe dimensions increase come from HOM addition in the field distribution. The small rounding radius  $r_b \sim 0.5r_h$  helps while keeping the effects of RF pulsed heating in tolerable limits. For L mode restrictions come from pulsed heating, require both larger hole rounding  $r_b \sim 1.5r_h$  and probe position in the place with smaller magnetic field.

## REFERENCES

- [1] X.J. Wang *et al.*, "Design and Construction a Full Copper Photocathode RF Gun", in *Proc. PAC93*, Washington, USA, May 1993, pp. 3000–3002.
- [2] B. Militsyn *et al.*, "Design of the high repetition rate photocathode gun for the CLARA project", in *Proc. LINAC14*, Geneva, Switzerland, Sep. 2014, pp. 1155–1157.
- [3] ANSYS, <http://www.ansys.com>.
- [4] V. Kulman, "Accelerating system", in *Ion linear accelerated*, B. Murin, Ed. Moscow, USSR: Atomizdat, vol. 2, pp. 36–46, 1978.
- [5] V. Paramonov and A. Skasyrskaya, "Pulsed RF heating simulations in normal conducting L-band cavities", DESY, Hamburg, Rep. TESLA-FEL 2007-04, 2007.
- [6] D. Pritzkau and R. Siemann, "Experimental study of rf pulsed heating on oxygen free electronic copper", *Phys. Rev. ST Accel. Beams*, vol. 5, p. 112002, 2002.
- [7] A.D. Kovalenko, *Introduction to thermoelasticity*, Kiev, USSR, Naukova dumka, 1965.